JOURNAL OF SANDWICH STRUCTURES & MATERIALS

Original Article

Journal of Sandwich Structures and Materials
2016, Vol. 18(3) 321–342

DOI: 10.1177/1099636215603036
jsm.sagepub.com
SAGE

Dynamic behavior predictions of fiber-metal laminate/aluminum foam sandwiches under various explosive weights

SB Baştürk[1], M Tanoğlu[2], MA Çankaya[3] and OÖ Eğilmez[3]

Abstract

Application of blast tests causes some problems to characterize the performance of panels due to the drastic conditions of explosive medium. Real test has high safety concerns and is not easily accessible because of its extra budget. Some approaches are needed for the preliminary predictions of dynamic characteristics of panels under blast loading conditions. In this study, the response of sandwiches under blast effect was evaluated by combining quasi-static experiments and computational blast test data. The primary aim is to relate the quasi-static panel analysis to dynamic blast load. Based on this idea, lightweight sandwich composites were subjected to quasi-static compression loading with a special test apparatus and the samples were assumed as single degree-of-freedom mass-spring systems to include dynamic effect. This approach provides a simpler way to simulate the blast loading over the surface of the panels and reveals the possible failure mechanisms without applying any explosives. Therefore the design of the panels can be revised by considering quasi-static test results. In this work, the peak deflections and survivabilities of sandwiches for various explosive weights were predicted based on the formulations reported in the literature. Major failure types were also identified and evaluated with respect to their thicknesses.

Keywords

Blast, testing, fiber/metal laminates, aluminum foam sandwiches

[1]Materials Engineering Department, Celal Bayar University, Muradiye Campus, Manisa, Turkey
[2]Mechanical Engineering Department, Izmir Institute of Technology, Gulbahce Campus, İzmir, Turkey
[3]Civil Engineering Department, Izmir Institute of Technology, Gulbahce Campus, İzmir, Turkey

Corresponding author:
SB Baştürk, Materials Engineering Department, Celal Bayar University, Muradiye Campus, 45040, Manisa, Turkey.
Email: bahar.basturk@cbu.edu.tr

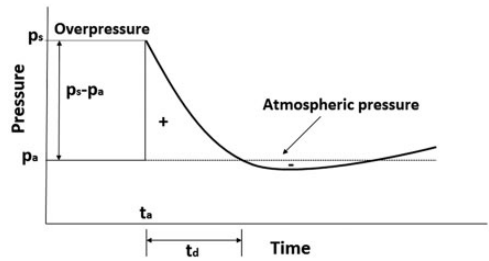

Figure 1. Pressure-time curve of idealized blast wave [1].

Introduction

For many decades, the performance of structures under blast loading has vital importance due to the presence of explosions and terrorist attacks. Drastic damage takes place where the explosions produce high pressure and loading rate such as structural failure, progressive collapse and extensive plastic deformation. Blast is a special kind of dynamic loading and created with the detonation of an explosive. Figure 1 shows the characteristic pressure-time of a blast wave. The t_a is the time for the arrival of the blast wave where P_s and P_a represent the peak pressure of the blast wave and ambient air pressure, respectively. The free-field pressure versus time behavior is generally expressed by a modified Friedlander formulation as given in equation (1). In this formulation, t_d is the positive phase duration and θ represents the time decay of the curve [2].

$$p(t) = (p_s - p_a)\left[1 - \frac{t - t_a}{t_d}\right]e^{-(t-t_a)/\theta} \tag{1}$$

The analysis of material systems against blast loading includes experimental work, theoretical modeling studies and numerical approaches. Application of the real blast test is not easily accessible due to safety concerns and high budgets. Various techniques are conducted to the material systems depending on the characteristics of blast conditions. Mostly used experimental facilities for replicating air blast loading are pressure blow down apparatus, impact testing with soft projectiles, shock tube facilities, medium-scale explosive detonations at large stand-off distances and small laboratory scale explosive detonations at small stand-off distances [1,3–5]. The deformation and fracture modes observed after blast loading have critical importance to reveal the structural response of the material systems. There are some studies related with the characterization of monolithic materials, fiber-metal laminate (FML) systems and sandwich structures under dynamic loading conditions. The researchers in the literature examined the metallic structures under different boundary conditions, various geometries and loading conditions. A number of failure modes of monolithic materials have been observed in blast experiments and these studies can be found in the literature [4,6].

Mouritz et al. [7,8] concentrated on the failure properties of glass fiber reinforced polymer (GFRP) composites which were subjected to under-water blast loading. Matrix cracking, fiber fracture and delamination were the main failure mechanisms observed after the tests. Reyes and Cantwel focused on the low-velocity impact properties of the FML systems that consisted of glass fiber reinforced polypropylene (GFPP) and aluminum (Al) metal layer [9]. Those tests showed that the FMLs with three different stacking sequence exhibited perfect resistance to dynamic loading. Reyes studied the impact performance of FML reinforced sandwich panels with Al foam core. It was found that the failure mechanisms of sandwich components contributed to the energy absorption capability of the system and the proposed energy balance model was in good agreement with the experimental results [10]. Zhu et al. investigated the blast response of Al foam core sandwich structures with metallic skins. Based on the experimental results, Al foam-based sandwiches' front faces exhibited localized failure on the centre part (tearing and indenting) and global deformation in the peripheral region. The back faces of the panels showed a uniform dome-shaped profile, moving out from the centre, varying a more quadrangular shape towards the clamped edges [11]. Huson et al. [12] have suggested a methodology which applies blast-like pressures and impulses to structures with complex geometry using non-explosive techniques. The most important superiority of that system is the implementation of realistic blast-like pressure/impulse versus time profiles without the use of explosives. Due to the complexity of dynamic loading conditions, some general assumptions have been made to understand the response of the materials under specific conditions. For simplification, the structure can be represented as either a single-degree-of-freedom system (SDOF) or multiple-degree-of-freedom system (MDOF) and the equilibrium equations are used for that reason [13]. Andrews and Moussa [14] evaluated the performance of sandwiches by combining experimental work and user-defined blast data. Based on that paper, to investigate the blast response of the sandwiches, the quasi-static sandwich panel analysis was related to dynamic blast loadings. The variation of face-sheet properties, panel aspect ratio (core/skin thickness) and core material type significantly affected the performances of the sandwiches. The analysis were evaluated by assuming the panel as an SDOF mass-spring system to include the dynamic effect [13,14]. The blast pressure was assumed to be almost uniform over the panel face. Core shear failure, face-sheet wrinkling/failure were considered as the main failure mechanisms. Compliance and natural frequency of the panels were calculated by using some special expressions to predict the final deflections of the panels under blast loading [14]. According to Reference 14, loading fixture for this test was established by considering the study of Reichard in 1992. Similar type of test frame was designed and tested by Wennhage and Zenkert to evaluate the performance of composite sandwiches under uniformly distributed transverse loading [15]. The presented test in this work is a preliminary version of hydromat test system (HTS) which has been developed as a structural test method for simply supported panels under uniform compression loading [16].

This article considers the sandwich samples with Al foams of various thicknesses in conjunction with skins composed of FMLs containing GFPP and Al sheet. The presented study has combined the experimental work for compliance determination and analytical approach for the dynamic deflection prediction. Effective compliance of the panels (C_p) was considered as constant and the related analysis were based on this assumption. Central deformations of the specimens were measured with linear variable differential transformer (LVDT) under compressive loading in order to determine the compliances of the sandwiches. By considering compliance parameter, the dynamic deflections of the panels under blast-type loading (depending on the explosive weight) could be predicted by manipulating the equation of motion – Newton's second law.

Theoretical modeling of structures under blast-type loading

In order to predict the response of materials under blast-type loading, some theoretical assumptions have been developed. These analytical assumptions enable the researchers to compare the parameters related with blast effect. The equivalent SDOF or mass-spring model is commonly used and achieves the fundamental response of the materials against dynamic loading which causes structural failure. The key terms to characterize the SDOF system are equivalent mass, damping and resistance function. In equations (2) and (3), the P^*, t, T, m and c represent the peak applied pressure (P_{blast} or P_{max}), time, effective blast wave duration (blast characteristic time), mass and damping coefficient, respectively [13]. The damping of the system under blast loading is ignored and the equation of motion becomes as expressed in equation (3).

$$mx'' + cx' + kx = p^*(t) \tag{2}$$

$$m\frac{d^2x}{dt^2} + kx = p^* e^{-t/T} \tag{3}$$

The schematic representation of SDOF system under static loading and linear oscillator loaded by a blast wave are shown in Figure 2(a) and (b), respectively. It should be noted here that the model described above is valid when the structure is deformed elastically. Based on the study of Baker et al. [13], the initial conditions of no displacement and no velocity at time $t=0$, $x(0)=0$ and $x'(0)=0$, respectively. After some manipulations, the final form of the equation of motion can be given as

$$\frac{x(t)}{P^*/k} = \frac{(\omega T)^2}{1+(\omega T)^2}\left[\frac{\sin \omega t}{\omega t} - \cos \omega t + e^{\frac{-\omega t}{\omega T}}\right] \tag{4}$$

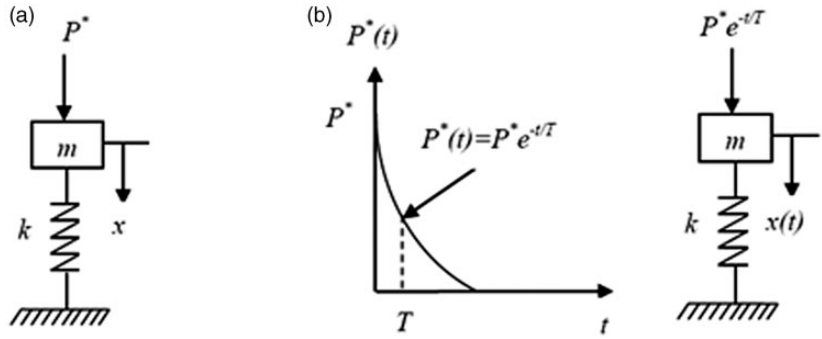

Figure 2. (a) Simple mechanical system under static loading, (b) linear oscillator loaded by a blast wave [12].

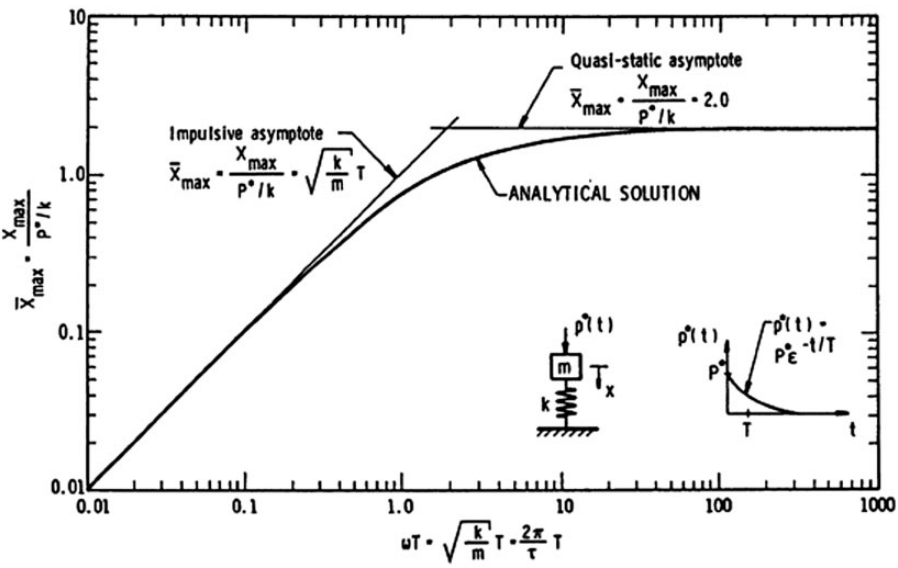

Figure 3. Characteristic function of SDOF system under blast loading [12,13].

The $\sqrt{k/m}$ is the natural frequency of the system and represented as (ω) in equation (4). In functional format, the transient solution given by equation (4) is reduced to

$$\bar{X}_{\max} = \frac{X_{\max}}{P^*/k} = \varphi(\omega T) \tag{5}$$

The trial and error solution to equation (5) is shown in Figure 3 and it characterizes the SDOF mass-spring system under blast loading [13,14]. Based on

reference [13], calculated $T\omega$ product was plotted and the resultant $\overline{X}_{\max}$ values can be determined. According to Figure 2(a), the deflection of the mass-spring system (δ_{static}) under P^* loading is equal to P^*/k. When the same system is subjected to dynamic blast loading, $P^* e^{-t/T}$, as indicated in Figure 2(b), the maximum deflection $X_{\max}$ becomes δ_{peak} and the ratio between them equals to the $\overline{X}_{\max}$, which is called as dimensionless deflection. Therefore, equation (5) can be modified as shown below in equation (6)

$$\overline{X}_{\max} = \frac{\delta_{\text{peak}}}{\delta_{\text{static}}} \tag{6}$$

Sandwich structures under blast-type loading

The sandwich panel deflection (δ_{static}) under maximum blast pressure (P^* or P_{blast}) was calculated by utilizing the constant effective compliance (C_p) formulation [14]. The compliance values of the sandwich samples were determined from the stress-central deflection graphs and for the required blast pressure, the corresponding δ_{static} values were calculated as described in equation (7)

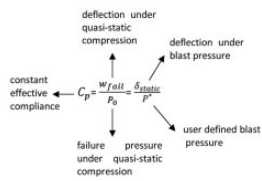

(7)

The peak deflection (δ_{peak}) of the panel under blast pressure was evaluated by considering the dynamic effect of the system, $f(T\omega)$ and formulated as in equation (8)

$$\delta_{\text{peak}} = \delta_{\text{static}} . f(T\omega) \tag{8}$$

The "T" is the blast characteristic time, "ω" represents the natural frequency for the lowest mode of the panel and given in equation (9). The related parameters like θ and ρ^* can be calculated by using equations (10) and (11) where the constants L_1 and L_2, E_f, h_f, h_c, d, ν_f, G_c, ρ_c and ρ_f represent panel dimensions (length and width), face-sheet elastic modulus, face-sheet thickness, core thickness, face-sheet and core thickness summation, face-sheet poisson ratio, core modulus, core density and face-sheet density, respectively [14].

$$\omega = \pi^2 \left[\left(\frac{L_2}{L_1} \right)^2 + 1 \right] \sqrt{\frac{\frac{E_f h_f d^2}{2\rho^* L_2^4 (1-\vartheta_f^2)}}{1 + \pi^2 \theta \left[\left(\frac{L_2}{L_1} \right)^2 + 1 \right]}} \tag{9}$$

$$\theta = \frac{E_f h_f h_c}{2G_c L_2^2 (1 - \vartheta_f^2)} \tag{10}$$

and

$$\rho^* = \rho_c h_c + 2\rho_f h_f \tag{11}$$

Blast-loading representation

The description of blast loading is based on the assumption that when the blast wave hits the structure it suddenly shows a peak pressure and then falls exponentially as seen in Figure 1. Regarding to the pressure-time *(P-t)* histories of panels, the blast characteristic time *(T)* describes the decay of the blast pressure and is calculated by using equation (12). In that formulation "P^*" represents the peak blast pressure ($P_{\max}$) and "t" represents the time [13,14].

$$P(t) = P^* e^{-t/T} \tag{12}$$

Fabrication of sandwich structures

In this study, FMLs containing GFPP and Al sheet were bonded together with Al foam cores for composing the sandwich panels. A closed-cell Al foam material (supplied by Shinko Wire Company Ltd, Austria) with the trade name ALULIGHT-AFS® was chosen as the core material and the foam panels contained about 0.6-mm thick non-porous Al skin that was produced during manufacture of the foam. The 500 × 500 mm Al foam structures were sectioned from larger panels of 8, 20 and 30 mm thicknesses and the cross sections of the panels are shown in Figure 4(a). The Al sheet/GFPP FML system and Al foam were integrated with PP-based film under 200°C and 1.5 MPa pressure and their schematic representations are shown in Figure 4(b). The produced sandwich structure was cut with a jigsaw and divided into four equal parts with the dimension of 250 × 250 mm.

Determination of mechanical and physical parameters

Both Al and GFPP components of the face-sheets were sectioned in the shape of dog bone and integrated with hot pressing technique at 200°C and 1.5 MPa pressure to obtain FML components of the sandwich samples. The tension tests of Al/GFPP skins were performed according to ASTM 8M-04 standard. The shear properties of the as-received Al foams were determined based on ASTM C273 standard. Both geometrical and mechanical/physical parameters calculated in

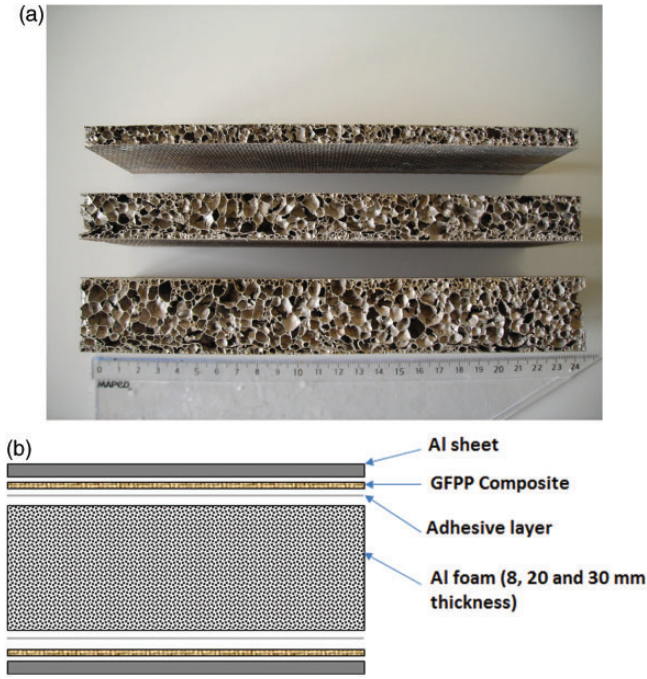

Figure 4. (a) As-received Al foam panels with 8-, 20- and 30-mm thickness. (b) Schematic representation of Al foam sandwich structures.

this study are given in Tables 1 and 2, respectively. The definitions of symbolic terms used in the tables are specified in 2.1.section.

Compression test of sandwich structures

The blast responses of the sandwich structures were predicted by relating the quasi-static analysis with dynamic blast loadings. For this purpose, the sandwich composites were subjected to compression loading with a specially designed loading fixture. The sandwich was considered as an SDOF mass-spring system that allows simulating the effect of blast loading on the panels. Although the constituents of sandwich panels (composite layer and Al foam) generally show strain rate sensitivity, this approach assumes that the dynamic responses of the panels do not dependend on the strain rate effects.The simply supported boundary conditions were assumed in the analysis and the distance between the supports was measured as 226 mm. The system had three main components: upper support frame, a liquid soap-filled rubber bladder and a lower frame. The sandwiches were located on the lower frame and the support frame acting as simple support boundary condition to the samples. The supports were made out of split cylindrical rods and welded on to the frame. Lower frame protected the sandwich and bladder during testing.

Table 1. Geometric properties of sandwich panels [3].

Sample type	L_1/L_2	h_f (mm)	h_c (mm)	d (mm)
8 mm Al foam sandwich	1	2.9	7.95	10.90
20 mm Al foam sandwich			17.90	20.80
30 mm Al foam sandwich			29.60	32.50

Table 2. Mechanical and physical parameters of sandwich panels [3].

Panel type	E_f (GPa)	G_c (MPa)	ρ_c (kg/m^3)	ρ_f (kg/m^3)	ν_f	θ	ρ^* (kg/m^2)	ω (N/m.kg)
8-mm Al foam sandwich	40.06	51	361.70	2512	0.32	0.17	17.44	3283.80
20-mm Al foam sandwich		18.50	330.40			1.04	20.48	2616.60
30-mm Al foam sandwich		20.10	388.20			1.59	26.06	2954.60

The liquid soap–filled rubber bladder was placed under the Al foam sandwich to provide uniformly distributed load over the surface of the panel. The pressure is controlled by operating the compression test machine; hence the variation of the load that presses the sample against bladder was monitored [3,15]. The linear variable differential transformer (LVDT) was used in order to detect the central deflection of the panels under compressive loading. An extra apparatus was manufactured to protect the LVDT measurement system and placed upon the upper support frame. A rigid steel plate was also located on to the LVDT protection apparatus to homogeneously distribute the load from the compression test head to the whole system. Technical illustration of the whole system is seen in Figure 5. The tests were conducted at room temperature with 250 kN loading cell using the Schimadzu^{TM} universal test machine at a crosshead speed of 5 mm/min [3].

Results and discussions

Effective compliance determination

Compliance expressions of the panels have critical importance for the blast loading analysis. The effective compliance term is defined as the ratio between the central deflection of the panel and corresponding applied pressure as indicated in equation (7) [14]. In our analysis, total central deflection terms of the panels were determined from the sensitive LVDT measurements and these results were used to determine

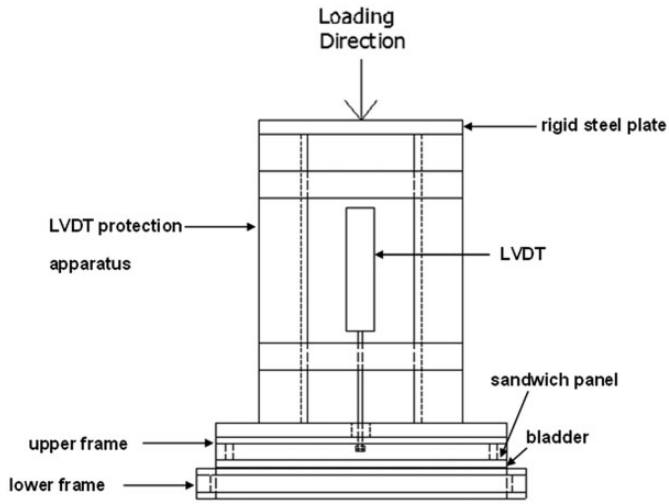

Figure 5. Technical illustration of compression test apparatus [3].

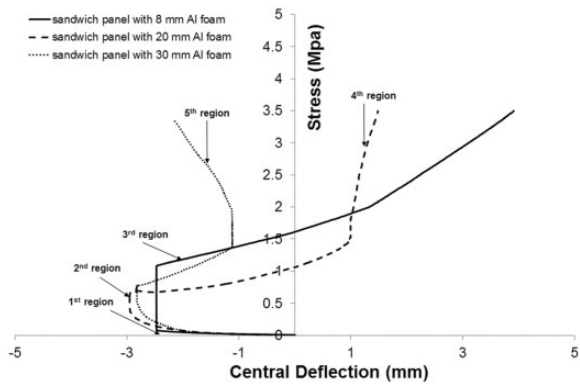

Figure 6. Stress versus central deflection graph of sandwiches with various thicknesses after compression test.

the final deflections under blast-loading conditions.The central deflection versus force data of Al foam sandwich panels during quasi-static tests were recorded and the stress was calculated by considering the area acting over the support frame. The typical sandwich panels for each thickness set of foam-based sandwiches were selected as representative cases and their stress versus central deflection behavior are given in Figure 6. For 8 mm Al foam sandwich, three distinct regions are visible on the graphs. In the first region, a linear deflection behavior is observed at low pressures. In the second zone, in spite of the stress increase, the central deflection is almost constant and in addition, thicker Al foam sandwich structures (20 mm and 30 mm foams) show extra regions. In the plots, the sample with 20-mm Al foams

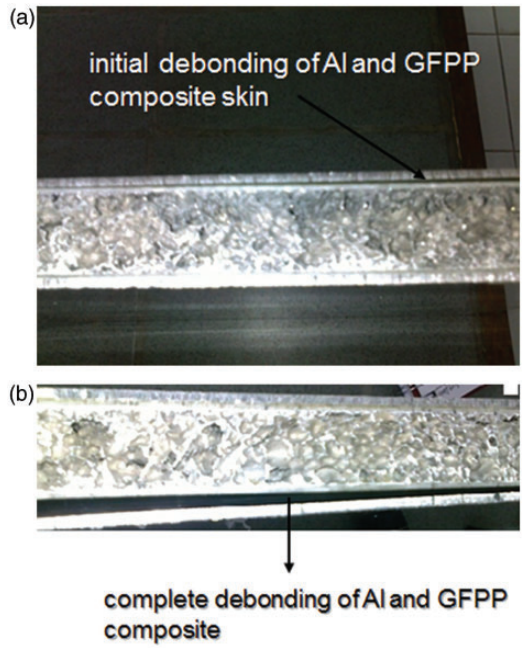

Figure 7. (a) Back-face view of the sandwich test panel with 20-mm Al foam at the end of 1st region. (b) Back-face view of the sandwich test panel with 20-mm Al foam at the end of 2nd region.

continue into 4th region at around 1.5 MPa pressure and the central deflection value is slightly changing. Similarly, the panel with 30-mm core exhibited five different zones during the test. In order to clearly identify the deformation modes and failure mechanisms of the panels the loading was interrupted at specific load level and the images of the deformed panels were captured. The photos of sandwich with 20-mm Al foam after the first and second region loading are shown in Figure 7(a) and (b), respectively. Based on these images and stress-central deflection plots, in the first linear part (1st region), the panel approached to bladder under compressive loading. The reaction force produced from the bladder was transmitted to the panel and initial debonding at the interface of the back-face sheet components (Al and GFPP) was observed during this zone as seen in Figure 7(a). In the second region, the bladder continued to push the sandwich sample and stress increase caused the complete separation of Al face-sheet from the whole panel. However, even at the final state of the second zone, GFPP composite currently bonded to the foam core as shown in Figure 7(b). Core shear or core crushing of Al foam was not observed during the 1st and 2nd regions and GFPP composite continued to protect the core material during these stages. The crushing of foam cells through the thickness of the panels started from the 3rd region and was not homogeneous during the compression. Therefore, the compaction of the whole sandwiches through the thickness

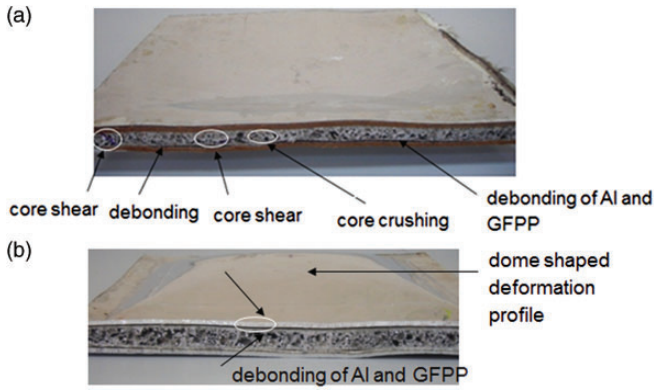

Figure 8. (a) Deformation patterns of sandwich panel with 8-mm Al foam and loaded up to 200 kN (front face view). (b) Deformation patterns of sandwich panel with 8-mm Al foam and loaded up to 200 kN (back-face view).

did not occur and some variations in foam compaction for the different zones of the panel were observed. When the central part reached its maximum compaction capacity, its deflection stopped; however, the zones around it continued to compact. Due to the collection of central deflection data, the graphs did not represent the whole sandwich structure deformation profile. As the core thickness increased, the repetition of this phenomenon was highly possible. Core shear and core crushing were the main failure mechanisms observed in the panels after the compression tests. In spite of the debonding between the FML components during the initial stages of the test, the protection of the core was performed by GFPP composite. Therefore, debonding of FML is not considered as the dominant failure mechanisms such as skin wrinkling or core shear. Independent of core thickness, all the samples exhibited similar type of deformation patterns and 8-mm Al foam sandwich is given as the representitive case in Figure 8. Both front-face and back-face views are presented and based on that figure, 8-mm foam structure showed relatively uniform deformation profile. The back face of the samples exhibited dome-shaped deformation moving out from the center, changing a more quadrangular shape towards the supported edges. Both Al foam core and front-face sheet gained an inwardly curved shape along the panel plane with the curvature extension. The average deflections of the panels after the compression test were measured and are given in Table 3.

Based on the tabulated results, the final deflections of the samples are not similar to the values obtained from the stress-central deflection graphs. This is attributed to the compliance effect of the bladder. Besides that, in order to reveal the pure bending behavior of a sandwich panel, its compression compliance must be known. In this study, the compliance corrections of the bladder (including test frame) and sandwiches were carried out by compressive loading of the bladder and sandwich panels under the same test conditions. After compliance correction, the real

Table 3. Average central deflection values measured after compression test.

Sample type	Average measured LVDT value (mm)
8-mm Al foam sandwich	17.36
20-mm Al foam sandwich	20.09
30-mm Al foam sandwich	19.45

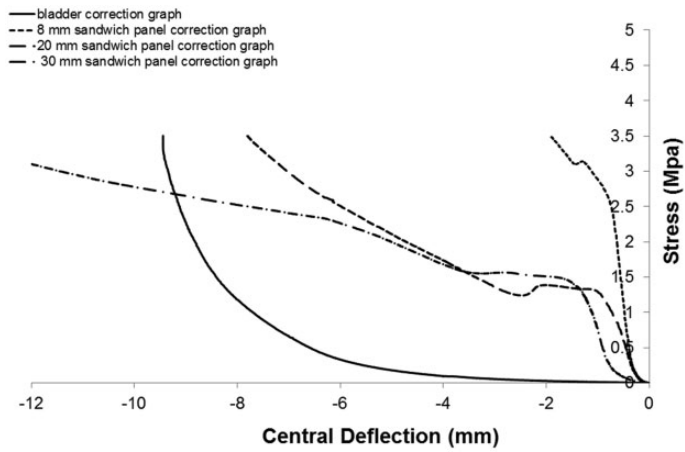

Figure 9. Compliance correction graphs of bladder and sandwich panels after compression test.

deflections of the sandwich structures were obtained. The central deflection data were provided by LVDT measurement equipment located on the upper rigid plate. The same system was also adopted for the bladder and their characteristic curves were constructed. The real central deflection values of the samples were calculated by subtracting the compliance deflection values of individual bladder and sandwich system from the compression test deflection values. Both the compliance curves of bladder and sandwich panels with various thickness are shown in Figure 9.

The identification of failure mechanisms has also great importance in terms of the compliance determination of the sandwich panels. After compliance correction, the compliance-corrected stress versus central deflection graphs of selected panels are shown in the Figure 10. The failure points of the panels were assigned as the starting of core crushing as indicated in the figure. In the literature, the compliances of the sandwiches can be evaluated based on the failure points of the panels [14]. For this study, the effective compliance (C_p) terms of structures were calculated by considering the central deflection (w_{fail}) and compressive pressure (P_0 or P_{fail})

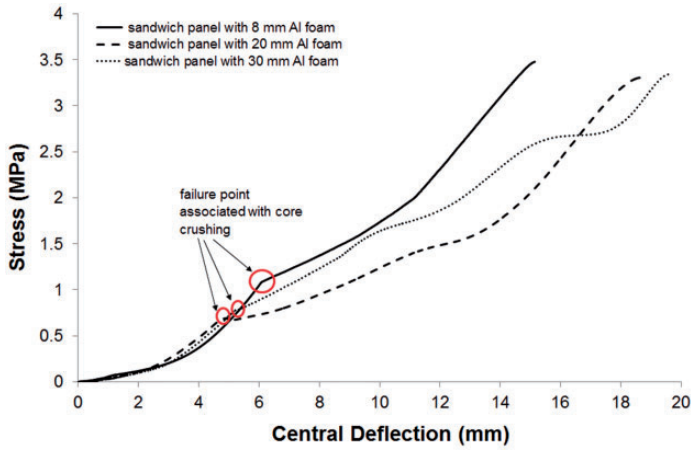

Figure 10. Stress versus central deflection plot of sandwich panels after compliance correction.

Table 4. Effective compliance values of sandwich panels after compression test.

Panel type	P_{fail} (MPa)	w_{fail} (mm)	Effective compliance-C_p (mm/MPa)
8-mm foam sandwich	1.00	5.89	5.87
20-mm foam sandwich	0.57	4.49	7.83
30-mm foam sandwich	0.67	4.89	7.12

values associated with core-crushing failure as formulated in equation (7). Based on the tabulated results given in Table 4, the 8-mm Al foam sandwich panel showed the minimum compliance as compared to the thicker structures. In addition to that, 20- and 30-mm foam panels exhibited very close compliance values.

Sandwich analysis under blast-type loading

Another important parameter used in this study is the blast characteristic time *(T)* to determine the peak deflection of the panel under blast pressure. Based on the pressure-time *(P-t)* histories of panels, the characteristic time term was calculated by using equation (12). Some numerical analysis was performed by using LS Dyna CONWEP module to determine the pressure-time histories of the blast loading [3]. Maximum blast pressures and corresponding characteristic time values together with other blast parameters are given in Table 5. Eight different TNT weights (12, 10, 8, 6, 4, 2, 1.37 and 1 kg) for 45 cm stand-off distance were selected as representative cases for the determination of blast parameters.

Table 5. Predicted blast parameters of panels with respect to TNT explosive amount for 45 cm stand-off distance.

Sample type	C_p (mm/MPa)	TNT amount (kg)	T (msec)	P^* (MPa)	$T\omega$ (N.msec/m.kg)	δ_{static} (mm)	$\overline{X}_{max}$	δ_{peak} (mm)
8-mm Al foam sandwich	5.8775	12	0.0367	15.64	120.52	91.95	1.974	181.55
		10	0.0384	14.43	126.09	84.82	1.976	167.60
		8	0.0333	13.11	109.35	77.06	1.972	151.97
		6	0.0322	11.39	105.74	66.93	1.971	131.91
		4	0.0285	9.64	93.59	56.64	1.967	111.41
		2	0.0288	6.88	94.57	40.44	1.968	79.58
		1.37	0.0345	5.45	113.29	32.03	1.973	63.19
		1	0.0292	4.89	95.88	28.72	1.968	56.51
20-mm Al foam sandwich	7.8290	12	0.0367	15.64	96.03	122.48	1.968	241.05
		10	0.0384	14.43	100.48	112.98	1.969	222.46
		8	0.0333	13.11	87.13	102.65	1.965	201.72
		6	0.0322	11.39	84.25	89.15	1.963	174.99
		4	0.0285	9.64	74.57	75.5	1.959	147.80
		2	0.0288	6.88	75.36	53.86	1.959	105.52
		1.37	0.0345	5.45	90.27	42.67	1.966	83.88
		1	0.0292	4.89	76.40	38.25	1.960	74.97
30-mm Al foam sandwich	7.1254	12	0.0367	15.64	108.43	111.47	1.971	219.72
		10	0.0384	14.43	113.45	102.83	1.973	202.87
		8	0.0333	13.11	98.39	93.43	1.969	183.96
		6	0.0322	11.39	95.14	81.14	1.968	159.68
		4	0.0285	9.64	84.20	68.67	1.963	134.79
		2	0.0288	6.88	85.09	49.02	1.964	96.28
		1.37	0.0345	5.45	101.93	38.83	1.970	76.50
		1	0.0292	4.89	86.27	34.81	1.964	68.38

As seen in tables, the maximum blast pressure was calculated as 15.64 MPa for 12 kg TNT explosive. The increase of TNT amount led to the increase of blast pressure, static and peak deflection parameters, as expected. The decaying characteristics of the blast pressure-time variation curve significantly affected the characteristic time term, T. Based on the tabulated results, the increase of T was not always proportional to TNT amount and showed its maximum and minimum values for 10 kg and 1 kg explosive weights, respectively. As indicated in the previous section, the $T\omega$ product is constructed as a function of $\overline{X}_{max}$ (dimensionless deflection) and is shown in Figure 3. In order to correlate $f(T\omega)$ and $\overline{X}_{max}$, the expression in equation (4) must be differentiated with respect to time t, and the resulting velocity set equal to zero to obtain the scaled time (ωt_{max}) when $x(t)$ is maximum. In that derived form, a transcendental type equation was obtained that

could be solved numerically. Once $\omega t_{\max}$ is obtained for specific values of $T\omega$, then $\omega t_{\max}$ could be substituted into equation (4) to obtain resulting $\frac{x_{\max}}{P^*/k}$ as a function of $T\omega$. In our study, both blast characteristic time (T) and maximum blast pressure (P^*) parameters were obtained based on P-t analysis. The natural frequencies of the sandwich panels with three different thicknesses were also calculated. The ωt values for each $T\omega$ product were calculated and the computed ωt was added into the equation (4) with corresponding $T\omega$ value. Hence, the $f(T\omega)$ was plotted and the resultant $\overline{X}_{\max}$ values can be determined. In our study the procedures mentioned above was performed via MATHEMATICA codes. The $\overline{X}_{\max}$ term is also given in the tables below and the details of this mathematical solution procedure are given in reference [3]. Although the dimensionless deflection of sandwich panels showed close similarities, the average $\delta_{\text{peak}}/\delta_{\text{static}}$ ratio of 8-mm Al foam sandwich specimen exhibited the maximum value. The peak deflections of the samples were calculated based on this ratio and are given in the same tables. As compared with the static and peak deflections of the panels for the same explosive weights, the 8-mm foam sandwich panel showed minimum values while the panel with 20-mm foam exhibited maximum deflections. The 20-mm and 30-mm Al foam sandwich panels showed the highest peak deflections of 241.05 mm and 219.72 mm for 12 kg TNT explosive, respectively. However, the deflection of 8-mm sandwich structure for the same weight was calculated as 181.55 mm. This situation is closely related with the natural frequency and compliance values of the sandwich structures. Independent of TNT amount, the 8-mm foam panel showed the minimum deflection while the 20-mm foam structure exhibited the highest deflection. This situation is attributed to the minimum δ_{static} value of the thinner panel because of its lower compliance. For the same blast pressures, the static deflection parameter showed a direct relationship with the compliance term. As this term decreases, the δ_{static} value also decreases.

The final step of this study is the determination of failure index. This index represents the ratio of peak deflection of the panel (δ_{peak}) under blast pressure to the deflection of the same panel (w_{fail}) under quasi-static compression loading (P_0) and expressed as in equation (13). The P_0 value can be defined as the onset of core shear or core crushing mechanisms and started at the end of 2nd region in central deflection-pressure graphs of sandwiches. If the failure index is greater than or equal to one the panel is predicted to fail, otherwise, the panel is assumed to survive [14].

$$\frac{\delta_{\text{peak}}}{w_{\text{fail}}} \leq 1 \; \textit{panel survives} \tag{13}$$

Table 6 shows the failure index values of the structures. The failure index aligned from the highest to lowest values by considering the corresponding blast pressures. Based on the tabulated results, none of the panels can survive. This is attributed to the high blast pressure values used in our analysis. The TNT weights utilized in this

Table 6. Predicted failure indexes of panels with respect to TNT explosive amount for 45-cm stand-off distance.

Panel type	w_{fail} (mm)	TNT amount (kg)	Predicted failure index (δ_{peak}/ w_{fail})
8-mm Al foam sandwich	5.89	12	30.80
		10	28.43
		8	25.78
		6	22.38
		4	18.90
		2	13.50
		1.37	10.72
		1	9.59
20-mm Al foam sandwich	4.49	12	53.61
		10	49.48
		8	44.86
		6	38.92
		4	32.87
		2	23.47
		1.37	18.66
		1	16.67
30-mm Al foam sandwich	4.89	12	44.91
		10	41.47
		8	37.60
		6	32.64
		4	27.55
		2	19.68
		1.37	15.64
		1	13.98

paper were selected based on the real threats; therefore, the present results have predicted the dynamic deflections under real conditions. Based on the test results and analytical predictions, the $f(T\omega)$ product has vital importance in terms of the failure of the panels. It can be concluded from Figure 3 that, for long blast durations (large $T\omega$ values) compared to the natural period of the system, the peak deflections arrive at a constant value equal to twice of the static deflection, δ_{static}. However, for short durations (small $T\omega$ values), the dimensionless deflection ($\delta_{peak}/\delta_{static}$) becomes equal to the $T\omega$ product and can be much lower than the constant value seen for large $T\omega$ values [13]. Therefore, the variation of T and ω significantly influence the dynamic deflection of the structure. Both blast pressure and impulse parameters directly affect the characteristic time of the blast wave.

Table 7. Geometrical parameters of reference studies.

	L_1/L_2	h_c (mm)	h_f (mm)	d (mm)
Wennhage and Zenkert[15]	1	25	1	26
Munoz[17]	1	25	2	27
Andrews and Moussa[14]	1	76.2	7.6	83.8

Similarly, the elements related with the natural frequency of the panel such as, E_f, h_f, d, G_c and ρ^* indirectly operate the dynamic response of the system. However, the panel dimension (L_1/L_2) ratio shows more considerable effect on the $f(T\omega)$ product compared to the other parameters. The increase of difference between the static failure pressure (P_0) and blast pressure (P^*) markedly change the δ_{static} of the sandwich structure. Under higher blast pressures, this difference becomes higher and when the $f(T\omega)$ is larger than one, the δ_{peak} will be greater than w_{fail} which leads to the increase of failure index. Thus, the survivability of the panel is highly dependent on these parameters mentioned above.

Comparison studies

In literature, there are only a few studies dealing with the coupling of quasi-static sandwich analysis and dynamic blast loading. The loading apparatus utilized in this work was a preliminary type of hydromat test (HMT) system so that we focused on the studies related with this test technique. Limited experiments with HMT are available with detailed panel information. The studies of Andrews and Moussa [14], Wennhage and Zenkert [15] and Munoz [17] were investigated as the reference papers and provided essential data to predict the blast parameters by using the SDOF mass-spring system approach. It should be emphasized that except reference [14], those studies did not examine the blast characteristics of sandwich structures so that there were no graphs/photos related with blast. The blast pressure (P^*) and characteristic time (T) values of various explosive weights available in our study were taken into account for comparison. Both geometrical dimensions and material properties of the panels which were introduced in the reference papers are listed in Tables 7 and 8, respectively. The analysis were carried out for 1 and 2 kg TNT weights *for 45 cm stand-off distance* and the resultant blast parameters are given in Table 9. Based on reference [15], under 78 kPa test pressure maximum central deflection (w_{fail}) of PVC core panel was 8.5 mm and the corresponding compliance (C_p) value was calculated as 108.97 mm/MPa. This ratio was assumed as constant and sandwich panel deflection (δ_{static}) under required blast pressure was obtained by using the C_p formulation as indicated in equation (7). The dynamic effect of the panel $f(T\omega)$ and related dimensionless deflection ($\overline{X}_{\max} = \delta_{\text{peak}}/\delta_{\text{static}}$) were computed with a MATHEMATICA code. Therefore, δ_{peak} values of the sandwich structures were calculated as expressed in equation (8). According to Table 9, the panels' peak deflections under blast pressures of 4.89 (for 1 kg TNT) and

Table 8. Material properties of reference studies.

	ρ_c (kg/m^3)	ρ_f (kg/m^3)	E_f (GPa)	G_c (MPa)	ν_f	C_p (mm/MPa)	ω (N/m.kg)
Wennhage and Zenkert[15]	100	2700	70	38	0.33	108.97	1333.90
Munoz[17]	80	1900	26	24	0.14	80.55	1986.60
Andrews and Moussa[14]	155	1900	20	189	0.18	639.64	239.10

Table 9. Predicted blast parameters of reference studies.

	TNT amount (kg)	T (msec)	P^* (MPa)	$T\omega$ (N.msec/m.kg)	δ_{static} (mm)	$\overline{X}_{max}$	δ_{peak} (mm)	w_{fail} (mm)	Predicted failure index (δ_{peak}/w_{fail})
Wennhage and Zenkert[15]	1	0.0292	4.886	38.95	532.50	1.922	1023.46	8.50	120.40
	2	0.0288	6.880	38.41	749.71	1.921	1439.45		169.34
Munoz[17]	1	0.0292	4.886	58.00	393.56	1.947	766.26	16.11	47.56
	2	0.0288	6.880	57.21	554.18	1.946	1078.44		66.94
Andrews and Moussa[14]	1	0.0292	4.886	6.983	3125	1.631	5096.87	142	35.89
	2	0.0288	6.880	6.887	4400	1.627	7159.52		50.42

6.88 MPa (for 2 kg TNT) were predicted as 1023.46 mm with 120.40 failure index and 1439.45 mm with 169.34 failure index, respectively. Similar type of trend was also valid for the study of Munoz. Based on that study, the predicted peak deflection of the PVC foam/glass fiber reinforce polymer structure for 1 kg TNT was calculated as 766.26 mm with 47.56 failure index. Andrews and Moussa searched four cases in reference [14] and only Case 1 was considered in this work for comparison. They investigated balsa foam core-based panel reinforced with E-glass fiber face-sheets and analyzed its response under blast-loading conditions. In that paper, the panel was represented as an SDOF mass-spring system to include the dynamic effect. They analyzed the response of the sandwiches under 91 kg TNT for 9.15 m stand-off distance and found the reflected pressure as 0.279 MPa with 698 kPa-ms impulse from reference [13]. Although the L_1/L_2 ratio was 1, the panel had 3.05 m width and 3.05 m length with 91.2 mm total thickness. Maximum central deflection (w_{fail}) and corresponding failure pressure (P_0) values were determined as 142 mm and 0.222 MPa, respectively. According to their analysis, the peak deflection of the system was 98 mm and the failure index was predicted as 0.69. When we adapted this panel to our blast conditions, dramatic results were obtained as seen in Table 9. At 4.89 MPa blast pressure, the predicted peak

deflection was 5096.87 mm with 35.89 failure index. At the same pressure for 8-mm Al foam sandwich analysis, corresponding peak deflection was estimated as 56.51 mm with 9.59 failure index. Both of those deflection and failure index values are higher compared to Al foam-based sandwiches. This may be attributed to the lower compliance and higher natural frequency of metallic foam panels.

Conclusions

In this study, blast responses of sandwich panels comprising Al foam and Al/GFPP FML system were predicted by combining the compression test results and user-defined blast data. The TNT weights were chosen by considering real threats; thus, the present results have predicted the dynamic deflections under real conditions. Core shear and core crushing were the main failure mechanisms observed in the panels after the test. Independent of core thickness, all the samples exhibited similar type of deformation patterns.

The effective compliance term of structures were determined by considering the central deflection and compressive stress values associated with core-crushing failure. The 8-mm Al foam sandwich panel showed maximum failure pressure (1 MPa) and minimum compliance (5.87 mm/MPa) values while the 20 - and 30-mm foam panels exhibited very close but lower compliance values as compared to the thinner structure. Both dynamic peak deflection and survivability of the sandwich panels were determined based on the results of compression test and related formulations. As compared with the static and peak deflections of the panels for the same explosive weights, the 8-mm foam sandwich panel showed minimum values while the panel with 20-mm foam exhibited maximum deflections. The 20-mm and 30-mm Al foam sandwich panels showed the highest peak deflections of 241.05 mm and 219.72 mm for 12 kg TNT explosive, respectively. However, the deflection of 8-mm sandwich structure for the same weight was calculated as 181.55 mm. This situation is closely related with the natural frequency and compliance values of the sandwich structures. It was computed that as the panel size increases both natural frequency and $T\omega$ product decreases. However, the ratio between maximum blast pressure and quasi-static failure pressure markedly influence the failure index of the structures. When this ratio becomes closer, the probability of surviving sandwiches increases.

Some related studies were selected from the literature to compare the blast characteristics of panels for 1 and 2 kg TNT weights. According to the tabulated results, as the lowest mode of natural frequency becomes higher the dimensionless deflection decreases. The compliance values of the foam panels given in reference works are larger as compared to the metallic Al foam panels, as expected. Based on the SDOF mass-spring approach, none of the panels could survive due to the higher dimensionless deflection values. In this study, we mentioned several thoughts on the comparison of blast test data with our predictions. It is hard to simulate the real blast-loading conditions to achieve exact peak pressure with accurate failure mode(s). The model described by Baker et al. [13] predicts the

elementary deformation mechanisms for a given design and user-defined blast data. Without using any explosives and special laboratory equipments the response of foam-based panels under blast-loading conditions were estimated via this approach. The predictions based on this model should be validated by performing medium-scale and/or small laboratory-scale explosive detonations.

Acknowledgements

The authors acknowledge TÜBITAK of Turkey for financial support under project 107A015 and Fikret ŞENEL from BARIŞ Elektrik Inc. of Turkey for contributions on the calculation of user blast data.

Declaration of Conflicting Interests

The author(s) declared no potential conflicts of interest with respect to the research, authorship, and/or publication of this article.

Funding

The author(s) received no financial support for the research, authorship, and/or publication of this article.

References

1. Zhu F and Lu G. A review of blast and impact of metallic and sandwich structures. *EJSE Special Issue: Loading Structures* 2007; 92–101.
2. Zhu F. *Impulsive loading of sandwich panels with cellular core*. PhD Thesis, Swinburne University of Technology, Australia, 2008.
3. Baştürk SB. *Development and mechanical characterization of anti-blast sandwich composites for explosive effect*. PhD Thesis, Izmir Institute of Technology, Turkey, 2012.
4. Jones N. Recent studies on the dynamic plastic behaviour of structures. *Mech Rev* 1989; 42: 95–115.
5. Langdon GS, Cantwell WJ, Guan ZW, et al. The response of polymeric composite structures to air blast loading: a state-of-the-art. *Int Mater Rev* 2014; 59: 159–177.
6. Nurick GN and Martin JB. Deformation of thin plates subjected to impulsive loading-a review, Part II: experimental studies. *Int J Impact Eng* 1989; 8: 171–186.
7. Mouritz AP. The damage to stitched GRP laminates by underwater explosion shock loading. *Compos Sci Technol* 1995; 55: 365–374.
8. Mouritz AP. The effect of underwater explosion shock loading on the flexural properties of GRP laminates. *Int J Impact Eng* 1996; 18: 129–139.
9. Reyes G and Cantwell WJ. The mechanical properties of fiber/metal laminates based on glass fibre reinforced polypropylene. *Compos Sci Technol* 2000; 60: 1085–1094.
10. Reyes G. Mechanical behavior of thermoplastic FML-reinforced sandwich panels using aluminum foam core. *Exper Model J Sandwich Struct Mater* 2010; 12: 81–96.
11. Zhu F, Zhao L, Lua G, et al. Deformation and failure of blast-loaded metallic sandwich panels-experimental investigations. *Int J Impact Eng* 2008; 35: 937–951.
12. Huson P, Asaro RJ, Stewart L, et al. Non-explosive methods for simulating blast loading of structures with complex geometries. *Int J Impact Eng* 2010; 38: 546–557.

13. Baker W, Cox P, Westine P, et al. *Explosion hazards and evaluation*. New York: Elsevier, 1983.
14. Andrews EW and Moussa NA. Failure mode maps for composite sandwich panels subjected to air blast loading. *Int J Impact Eng* 2009; 36: 418–425.
15. Wennhage P and Zenkert D. Testing of sandwich panels under uniform pressure. *J Test Eval* 1998; 29: 101–108.
16. Melrose P, Lopez R and Muszynski L. Elastic properties of sandwich composite panels using 3-D digital image correlation with the hydromat test system. In: *SEM X international congress & exposition on experimental & applied mechanics*, Paper No.490:7, 2004.
17. Munoz S. Structural health monitoring using embedded fiber optic strain sensors. PhD Thesis, University of Maine, USA, 2008.